Accepted Manuscript

Hydrogen bonds autonomously powered gelatin methacrylate hydrogels with super-elasticity, self-heal and underwater self-adhesion for sutureless skin and stomach surgery and E-skin

Bingcheng Liu, Ying Wang, Yong Miao, Xinyu Zhang, Zhexiang Fan, Gurankit Singh, Xingying Zhang, Kaige Xu, Bingyun Li, Zhiqi Hu, Malcolm Xing

PII: S0142-9612(18)30279-5

DOI: 10.1016/j.biomaterials.2018.04.023

Reference: JBMT 18609

To appear in: *Biomaterials*

Received Date: 28 February 2018

Revised Date: 8 April 2018

Accepted Date: 12 April 2018

Please cite this article as: Liu B, Wang Y, Miao Y, Zhang X, Fan Z, Singh G, Zhang X, Xu K, Li B, Hu Z, Xing M, Hydrogen bonds autonomously powered gelatin methacrylate hydrogels with super-elasticity, self-heal and underwater self-adhesion for sutureless skin and stomach surgery and E-skin, *Biomaterials* (2018), doi: 10.1016/j.biomaterials.2018.04.023.

Hydrogen Bonds Autonomously Powered Gelatin Methacrylate Hydrogels with Super-elasticity, Self-heal and Underwater Self-adhesion for Sutureless Skin and Stomach Surgery and E-Skin

Bingcheng Liu[a,b#], Ying Wang[c#],Yong Miao[a],Xinyu Zhang[a], Zhexiang Fan[b], Gurankit Singh[b], Xingying Zhang[b], Kaige Xu[b], Bingyun Li[d], Zhiqi Hu[a*], Malcolm Xing[a,b,c*]

[a] Department of Plastic and Aesthetic Surgery, Nanfang Hospital of Southern Medical University, 1838 North Guangzhou Avenue, Guangzhou, Guangdong 510515, China

[b] Department of Mechanical Engineering, University of Manitoba, Winnipeg, MB R3T 2N2, Canada

[c] Institute of Burn Research, Southwest Hospital, Army Medical University, Chongqing, 400038, China

[d] Department of Orthopaedics, School of Medicine, West Virginia University, Morgantown, WV 26506, USA

same contributions

*:corresponding author: malcolm.xing@umanitoba.ca (MX);
doctorhzq@hotmail.com (ZH)

Abstract

Interface-interaction induced self-healing and self-adhesive are a gem–like attribute inspired by our Mother Nature. Biocompatible gelatin methacrylate (GelMA) hydrogels exhibit tunable mechanical properties which are favorable in biomedical applications. However, it is difficult to integrate high stiffness, super-elasticity, large deformability and self-healing property together. Here, we report a GelMA-based double-network (DN) hydrogel with above properties by utilizing tannic acid (TA) as a multi-functional H-bond provider. We first investigated the morphological and mechanical properties' changes of GelMA over different TA's concentrations and treating times. In comparison to pristine GelMA hydrogel (10% w/v), the GelMA-TA hydrogels presented significant increase in ultimate stress (4.3-fold), compressive modulus (2.5-fold), and especially in elongation (6-fold). Adhesion properties of GelMA-TA can be tuned by TA and have been proven to be water-resistant. To test gels' feasibility *in vivo*, we applied GelMA-TA gels to close skin wound and gastric incision without suture. The results indicated the gels had the capabilities of promoting wound healing with superior tissue restoration and minimal tissue adhesion. Furthermore, integrated with carbon nanotubes, the GelMA-TA-carbon nanotube gel was an alternative self-healing electric skin with strain-sensitive conductivity. This work demonstrated a strategy to yield

mechanically strong hydrogel adhesives for innovative biomedical applications.

Keywords:
Tannic acid induced double-network gelatin gel, Superelasticity, Self-healing, Tissue adhesive, Sutureless surgery, Biosensor

1. Introduction

As the microstructures and biological properties are akin to the extracellular matrix of native tissues, hydrogels play a vital role in tissue engineering and regenerative medicine. [1] Besides these fundamental purposes, hydrogels are also a promising candidate to engage in novel biomedical applications, such as wound dressings.[2-4] However, our bodies are extremely sophisticated, for instance, even a small piece of skin on hands, they can sustain deformation, sense objects and restore from scratch, which simulating in hydrogels are flexibility, pressure sensibility, and self-healing attribute. Thus, the simple strategies to access multi-functional and biocompatible hydrogels are always being pursued.

Denatured from collagen, Gelatin is a less expensive protein-based hydrogel biomaterials. They have the superior biocompatibility than synthetic due to the intrinsic natural fibril structures and bioactive cues,[5, 6] as well as present relative low antigenicity compared to collagen.[7, 8] Despite these advantages above, chemical cross-linkers, for example, glutaraldehyde, are needed to obtain stable hydrogel networks. Nevertheless, an alternative option is always welcomed to avoid the cytotoxicity of residues and possibly long-term calcification in vivo after conventional chemical gelation.[9, 10]

Modification of gelatin by grafting methacryloyl moieties on amine groups of lysine generates gelatin methacrylate (GelMA).[11, 12] Manipulating mechanical properties of Gel-MA by adjusting the degree of methylation (DM) and concentration of GelMA are well studied among tissue engineering.[13, 14] The real dilemma is that the most of existing methods can only improve hydrogel performances on the one aspect. For example, aiming to better the compressibility of GelMA hydrogel, the cryogenic process yielded flexible and macroporous interconnected network via ice crystal sublimation. Whereas, it sacrificed the elastic modulus or extensibility.[15]

The hybrid gel is an approach to handling the pluripotency on functions, by selectively adding functional components. GelMA-based hybrid hydrogels have been intensively studied by incorporating inorganic nanoparticles,[16, 17] and polymers[18, 19]. These mechanically adjustable GelMA DN gels have led

to the success in creating the favorable extracellular matrix (ECM) for specific tissue reconstruction[20, 21] or meeting the demand for biofabrication technology such as photolithography, microfluidic or 3D printing.[22, 23] However, synthesis of a hydrogel that can couple favorable mechanical with enticing interactive properties is still challenging.[24]

Learning from nature (e.g., skin epidermis regenerates after injury, or mussels can firmly attach to the rock withstanding waves) is an effective way to acquire the desired results.[25-27] Specifically, Tannic acid(TA) is a natural plant source polyphenols compound that intrinsically exhibits biological antioxidant and antibiosis properties.[28] Besides, extensively innovative studies have engaged TA as building blocks to construct layer-by-layer self-assembly films or multilayer nanoparticles by utilizing its versatile binding capabilities.[29-31] Nevertheless, it still encounters tough challenges to manipulate the strong interactions between TA and biomacromolecules in the construction of bulk hydrogels, since they always tend to form the amorphous structure of complex or coagulation.[32-35] The existing strategies to seek the balance of the interactions by either selecting particular biomacromolecule (e.g., DNA),[36] or adopting multi-step operations under precisely controlled conditions.[33, 37] What is more, similar to mussel-inspired biomaterials, high content anchor moieties (catechol and pyrogallol) in TA's molecular structure can bestow composite hydrogels with tissue-like self-heal ability and adhesiveness to diverse surfaces.[38-40]

Here, to make full use of TA's excellent bonding ability to generate innovative GelMA-based double-network (DN) hydrogel, we hypothesize that a pre-crosslinked GelMA hydrogel network not merely can be strengthed by TA in a well-arranged manner, but also provide a platform for TA to perform its adhesive properties. Specifically, we firstly verified the formation of and defined the optimal chemical composition of GelMA-TA hybrid hydrogels. The improvements of compressive and tensile properties were then tested. After that, interfacial interactions of hydrogels (self-healing and adhesiveness) were systematically evaluated, and the wet adhesion ability was highlighted. Subsequently, we conducted *in vivo* experiments to demonstrate the capability of hydrogel for the closure of surgical incision in two forms, anti-tensile healing (skin), and body fluid tolerant healing (gastric). Finally, the GelMA-TA hydrogel with multiple wall carbon nanotubes (MWCNTs) was tested as a wearable strain-sensitive E-skin.[41, 42]

2. Results and discussion

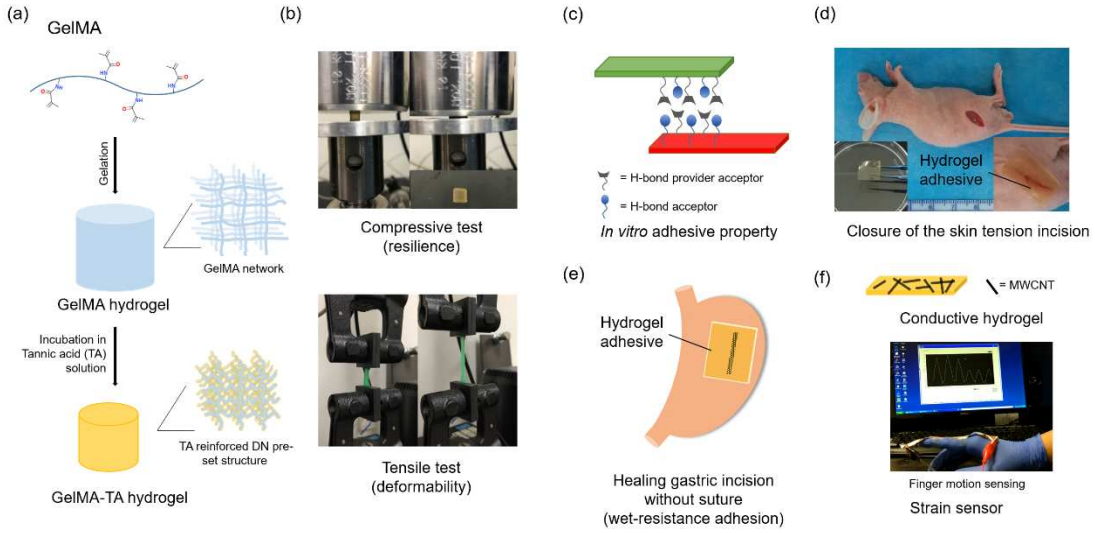

Scheme 1. The schematic illustration of preparing multifunctional GelMA-TA hydrogel (a) with high stiffness, super-elasticity, deformability (b), and *in vivo* self-healing and adhesive property (c). Biomedical applications of GelMA-TA gel for skin wound closure (d), sutureless gastric surgery (e), and applied as strain sensor with the presence of MWCNTs (f).

2.1 Formation of GelMA-TA hydrogel

We synthesized pristine GelMA hydrogels with different concentration by following a well-established method.[13, 43] As shown in Fig. 1a, after a 24 h treatment of TA (100% w/v), the transparent GelMA hydrogels (cylindrical shape with 7 mm in height and 7 mm in diameter; 10, 15, 20% (w/v)) turned into translucent along with size reduction, which shows the substrantial interactions between TA and GelMA. The Fourier Transform Infrared (FT-IR) studies were performed to measure the interactions (Fig. 1b). The spectra of GelMA-TA showed a typically wave at around 3100-3600 cm^{-1} are closely related to the formation of hydrogen bonds due to the wavenumber of amine N-H and galloyl O-H shift in this range.[44, 45] The peak value 3309 cm^{-1} (GelMA) shifted to 3269 cm^{-1} (GelMA-TA) indicated the formation of H-bonding.[46] Furthermore, characteristic peaks of GelMA hydrogel (amide I, amide II, amide III) [47] were routinely observed at around 1612 cm^{-1}, 1520 cm^{-1}, and 1436 cm^{-1}, without distinct change of intensity and frequency. This result also provided evidence that there was no existence of covalent bonding.

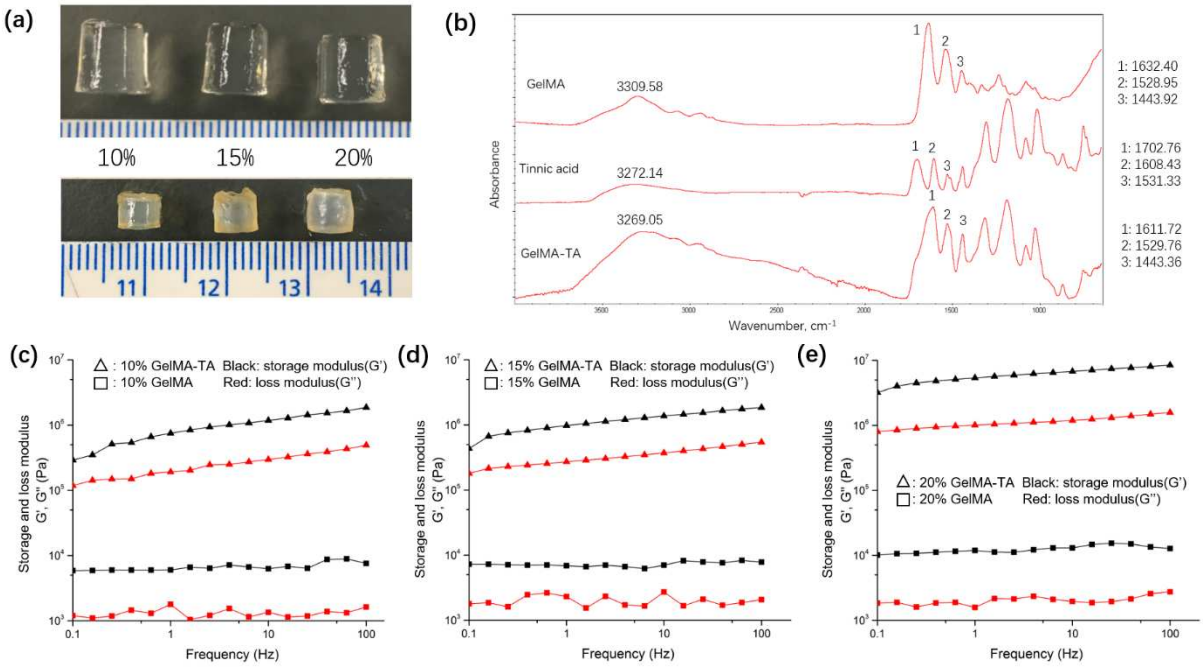

Fig.1 (a) The representative morphological changes from pristine GelMA hydrogels (upper) to GelMA-TA (bottom) after a 24h incubation in TA solution. Concentrations of GelMA and TA are 10%, 15%, 20% (w/v), and 100% (w/v), respectively. (b) FT-IR spectra of 10% GelMA (upper)), 100% TA (middle) and as-prepared GelMA-TA (bottom). (c-e) The rheological properties of GelMA-TA hydrogels (triangle) and corresponding GelMA pristine hydrogels (block). Concentrations of GelMA from left to right are 10%, 15% and 20%. G': Storage modulus (black), G": loss modulus (red).

2.2 Mechanical properties

The dynamic mechanical properties of GelMA-TA hydrogels were evaluated by rheological experiments. We divided GelMA-TA and corresponding GelMA hydrogels into three groups according to the concentration and swept at room temperature with predetermined oscillation frequency. First of all, storage modulus (G') was higher than loss modulus (G") in all samples (Fig.1c, d, e) without any crossover traces occurred, which indicates the formation of stable hydrogels. With the increasing concentrations of GelMA, storage modulus (G') in all groups were climbing. Specifically, either G' or G'' of GelMA-TA were significantly higher than pristine GelMA, which suggests the mechanical properties of GelMA-TA are stronger. Notably, unlike the flat traces of GelMA, a meaningful elevation of storage modulus (G') of GelMA-TA was observed, and could be explained as an indication related to the presence of non-covalent bonds in the hydrogel.[36, 48]

The mechanical strength of adhesive hydrogels is important for maintaining structural integrity during their work period. Thus, TA's effects on the mechanical performances of gels were systematically evaluated. In Fig. 2a

and b, the ultimate stress of GelMA-TA hydrogels (4.6 MPa for 20% GelMA-TA and 3.2 MPa for 10% GelMA-TA) were considerably increased compared to the corresponding pristine GelMA, which were up to 3.5, and 4.3 folds of the latter, respectively. The same trend was found in both compressive modulus (Fig.2c) and tensile properties (Fig. 2e, f), indicating that we succeeded in obtaining a stiffer hydrogel. Moreover, deformability, the inferior part of GelMA's performance, has been greatly improved. We found TA treated GelMA gel led to a far better elongation than that of the pristine counterpart, especially in GelMA with high DM.[49] The elongations of GelMA-TA hydrogels (277%, 225%, and 154%) with growing GelMA concentrations (10%, 15%, 20%) were at least around 6, 6 and 5 folds higher than those of the previous report.[43] However, the compressive and tensile strain decreased with increasing initial concentration of GelMA, especially in 20% groups (Fig. 2d, e). This phenomenon was considered caused by the combined effect of volume reduction of hydrogels and high crosslink density which consequently led to a brittle polymeric chain.[50, 51] Taken together, we chose 10% GelMA-TA for subsequent studies since it renders the best elongation as well as the comparable mechanical performances to skin and soft tissue.[52, 53]

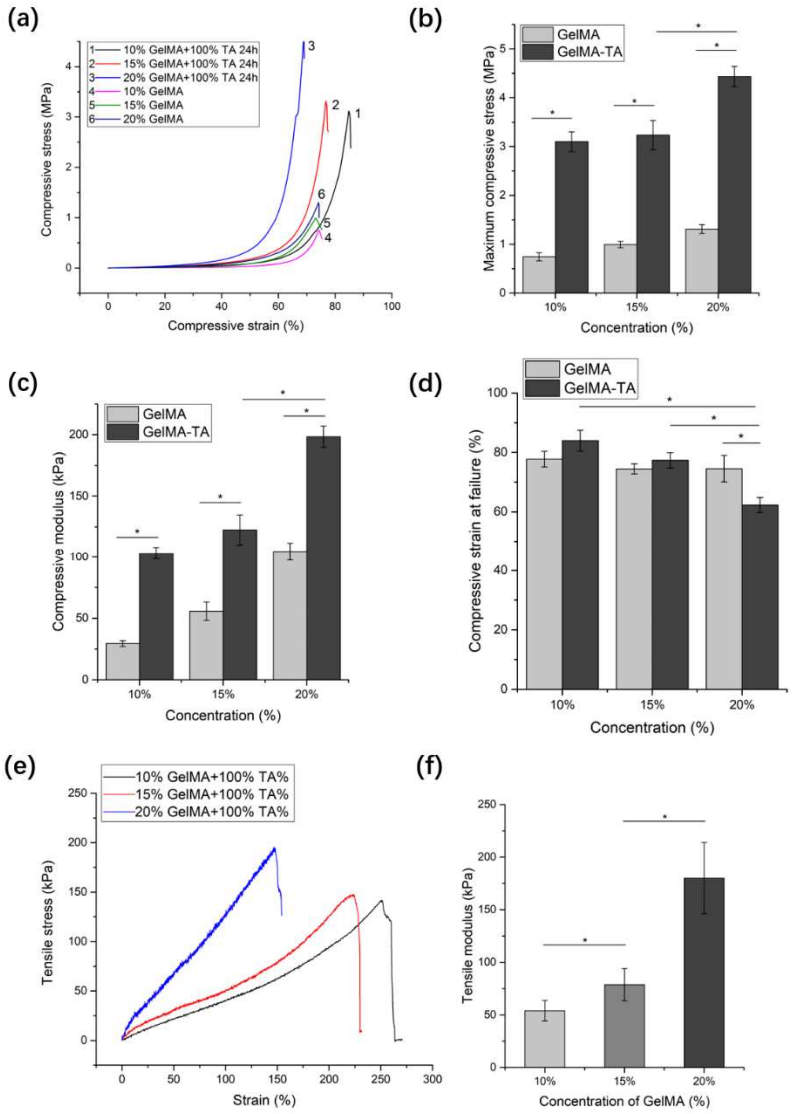

Fig. 2: The mechanical properties of 10%, 15% and 20% GelMA and corresponding GelMA-TA (100% w/v TA, 24h treatment time). The compressive curves (a), maximum compressive stress (b), compressive modulus (c), and compressive strain at failure (d) of GelMA-TA hydrogels. The tensile stress-strain curves (e), and tensile modulus (f) of GelMA-TA hydrogels. (* indicates significant differences, $p < 0.05$, n=3)

For further investigations of the effects of TA' s concentration and acting time on gel's mechanical properties, we selected 100%, 60%, 30% (w/v) TA and 3h, 6h, 12h, 24h, and 48h treatment time as variables. As in Fig. 3a, b volume shrinking rate of GelMA-TA to GelMA were proportional to the TA concentration and treating time in all groups. This phenomenon is similar to the previous reports that TA/macromolecule ratio determine the intension of

interactions.[34, 35] The maximum compressive stress was also in response to the variables (Fig. 3c). Specifically, Compressive stress in 100% TA group reached the peak at 24 h and was no longer significantly changing at 48 h, whereas, the stress in 60% group gradually elevated along with time but could not reach the level of 100% group even at the end of 48 hours and the irregular changes was found in 30% group. We then identified the difference between two 100% GelMA-TA hydrogels with 24h and 48h treatment time via deformation recovery abilities. After five successively compressive cycles at 80% strain, the recovery ratio in the height of two gels were 90% and 78%, respectively (Fig. 3d; Movie S1, Supporting information). The reduction of resilience was considered as the plasticization effect of TA which probably related to the prolonged exposure.[54, 55] Swelling ratios of hydrogels were characterized and were shown in Fig. 3e. Macroscope of GelMA-TA have shown that the H-bonding interactions between TA and GelMA compressed the structure of hydrogels, which in turn might limit their water loading capacity. As expected, all GelMA-TA hydrogels swelled significantly lower than pristine GelMA. Other findings also demonstrated that the increased TA concentrations could lower the ratio, which was consistent with the mechanical performances due to the denser H-bonding networks. It is believed that hydrogels with relatively low swelling behavior also exhibited prolonged degradation rate, thus could extend the functional lifetime of hydroges.[43, 56] Taken together, we settled 100% TA and 24h as well-defined treatment conditions for the following studies.

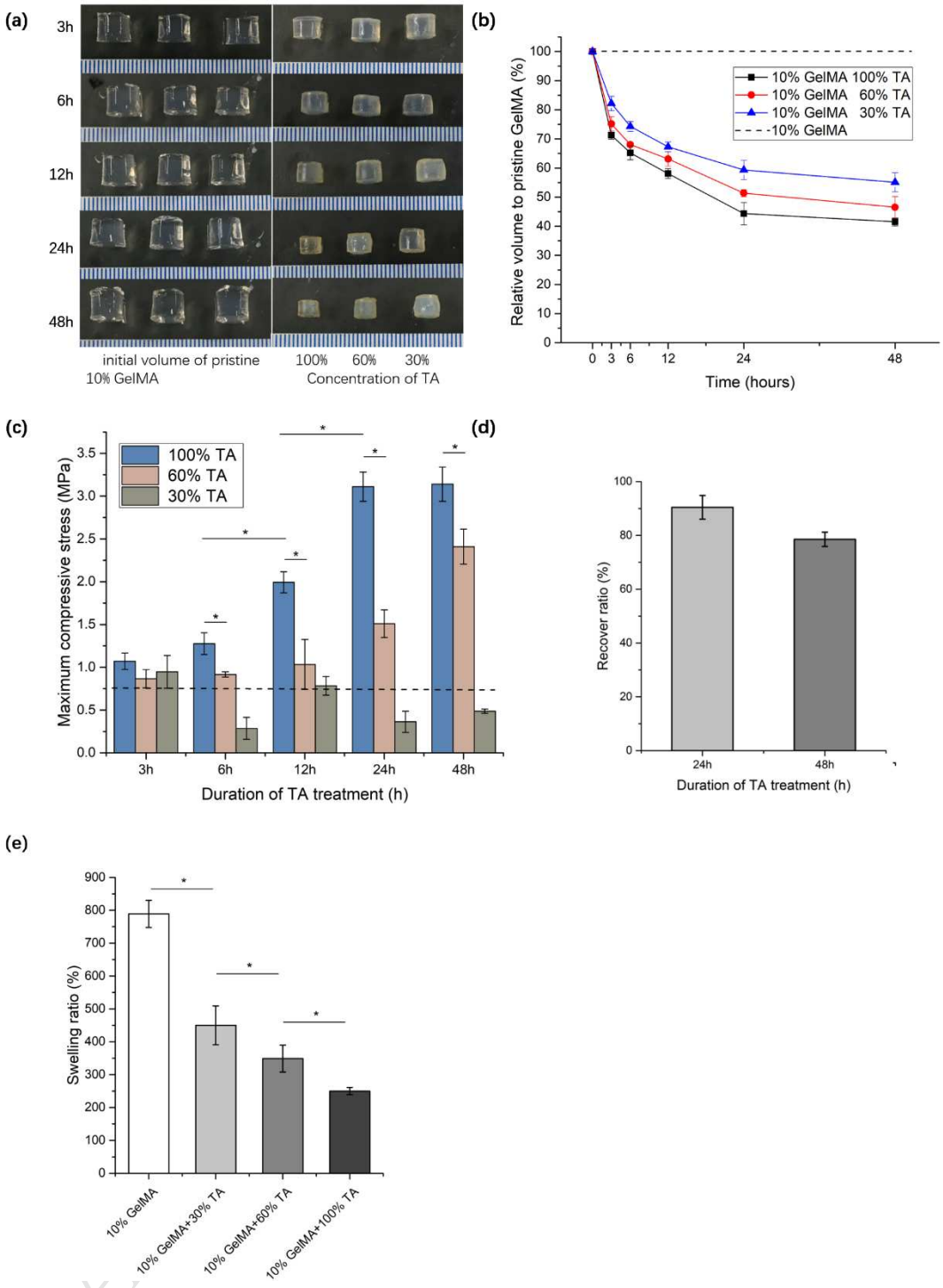

Fig. 3 (a) Representative photographs of 10% GelMA hydrogels (left) and GelMA-TA hydrogels after treatments over different concentrations of TA and durations (right). (b) The relative volume curves of GelMA-TA hydrogels compared to their original volume (GelMA). Dash line indicates the volume of GelMA as 100%. (c) Time-dependent and TA concentration-dependent changes in maximum compressive stress of GelMA-TA hydrogels. Dash line refers to the maximum compressive stress of 10% GelMA hydrogel. (d) Recovery ratio of two different GelMA-TA hydrogels in the height

measurement after five consectively compressive cycles at 80% strain. (e) Swelling ratio of GelMA and GelMA-TA hydrogels. (* indicates significant differences, $p < 0.05$, n=3)

2.3 Morphological study

From SEM observations, the pristine GelMA hydrogel (Fig. S1a) exhibited a honeycomb-like porous microstructure ascribed to the evaporation of water.[57, 58] However, after treatment of TA, we found thickened cell walls and a reduction of average pore size from 22.8 μm (GelMA) to 9.8 μm (GelMA-TA) (Fig. S1b, c). It suggests that GelMA's covalent networks can effectively withstand the strong H-bond interactions, which leads to general shrinkage rather than cell collapse. From this perspective, as the second network of the hydrogel, TA contributes a pre-set structure to GelMA. Their synergistic effect gives gel unparalleled mechanical properties in GelMA-based hydrogels.

2.4 Tissue adhesion

Adhesion of GelMA-TA hydrogels to various substrates was demonstrated in Fig. S2. Hydrogels in two shapes (cylinder or thin sheet) were able to generate sufficient adhesiveness on rubber, plastic, metal, and glass. Notably, two pieces of glass slides jointed by hydrogel could withstand extra weight not less than 500g. For biomedical aspect, we applied porcine skin as representative tissue for quantitative examinations. The set up of the specimen for shear adhesion tests were illustrated in Fig. 4a. In Fig. 4b, the highest adhesive strength was found in 100% TA group at 81 kPa, which was significantly superior to those in lower concentration groups and two control groups (10% GelMA and fibrin glue as in our previous publication.[59] Though TA inherently presented adhesiveness, it was not commensurate to GelMA-TA's, which is probably owing to the instability of the amorphous structure. Force-distance curves were plotted to evaluate the performances of hydrogels with the thickness of 0.3mm or 1mm (Fig. 4c). Thick gel showed superior elongation while maintaining the adhesion. The elongation of the thick gel group was up to 5.8 mm. By contrast, the elongation of thinner gel and 100% TA were up to 4.5 mm and 2.4 mm, respectively. It is a crucial ability of tissue adhesives that offering flexibility to accommodate deformations of tissue under physiological condition while maintaining robust adhesion strength.[60] Therefore, 1 mm thick hydrogels were chosen for the following *in vivo* experiments.

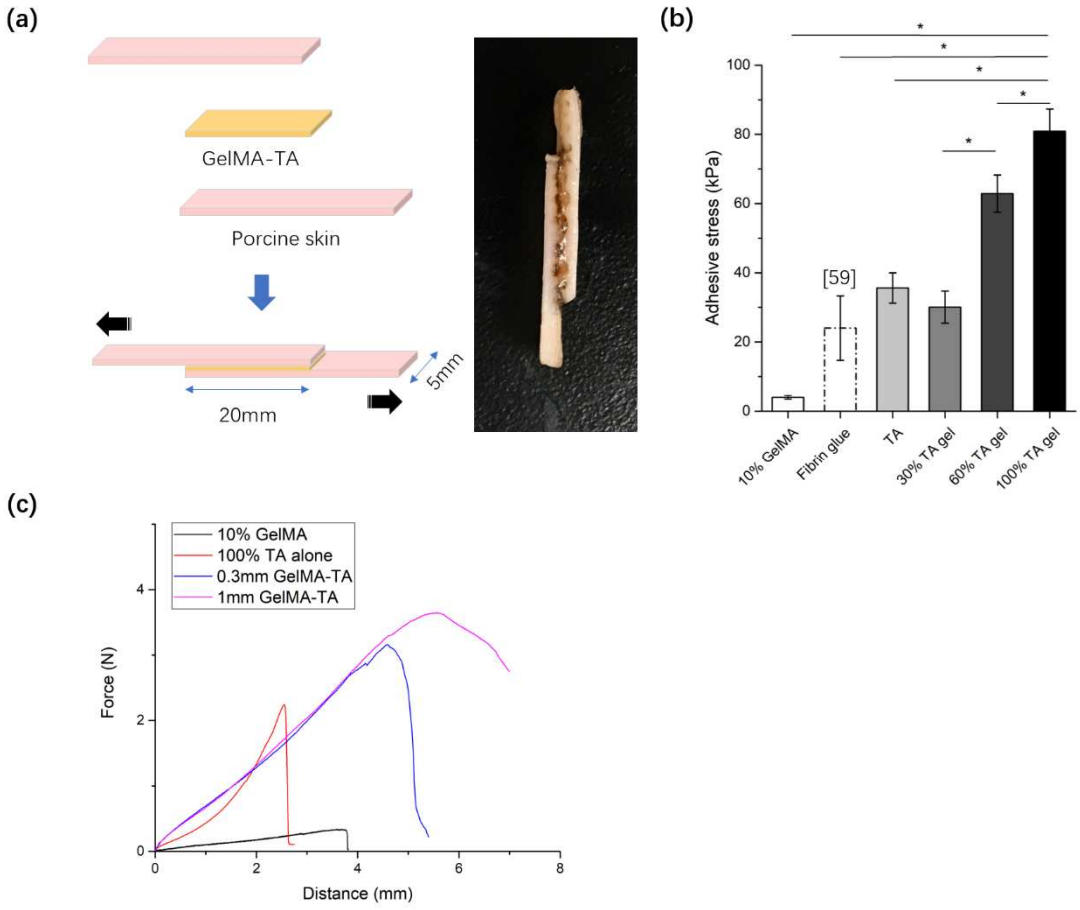

Fig. 4 (a) Schematic and representative photograph of prepared specimen for shear adhesion test. (b) Adhesion strength of 10% GelMA, fibrin glue (From our previous publication [59]), 100% TA and GelMA-TA hydrogels under three different treatment conditions to porcine skins. (* indicates significant differences, $p < 0.05$, n=3) (c) Shear-distance curves.

2.5 Self-healing model

Self-healed hydrogels were used to deepen the understanding of hydrogel adhesiveness before *in vivo* applications. As shown in Fig. 5a, to prepare hydrogels, two gel pieces reconnected in either head-to-head or overlap forms. The junction primarily took place after applying a gently external pressure for 1 minutes (Movie S2, Supporting Information). Then the hydrogels were undergoing a 6h strengthening process. Evaluations were performed as tensile tests (Fig. 5b; Movie S2, Supporting Information). There were no significant differences in mechanical properties between rebonded and pristine GelMA-TA hydrogels (Fig. 5c). Also, the adhesion strength between two hydrogels was strong enough, because so far in our experiments, no fracture occurred at the joint.

To confirm the driving force, we immersed hydrogel in urea solution since it can disrupt the existing hydrogen bonds in the hydrogel.[61] Indeed, two hydrogels separated spontaneously and the whole process completed within 20min (Fig. 5d). In contrast, separation did not occur when water presented along (data no shown). The bonding ability of bioadhesives to tissue in a wet environment is of importance but challenge the researchers a lot.[62, 63] We further tested the water-resistant adhesion property of GelMA by applying the same healing model, and a 7-day observation period was carried out in the phosphate buffer solution (PBS). It was found that the hydrogel was maintaining a constant connection throughout the entire observation period (Fig. 5e; Movie S3, Supporting Information). PBS solution is expected to simulation the body fluid due to the similar osmolarity. Therefore, the swelling properties of hydrogel might not be the key factor to affect the stability of bonding *in vivo*.

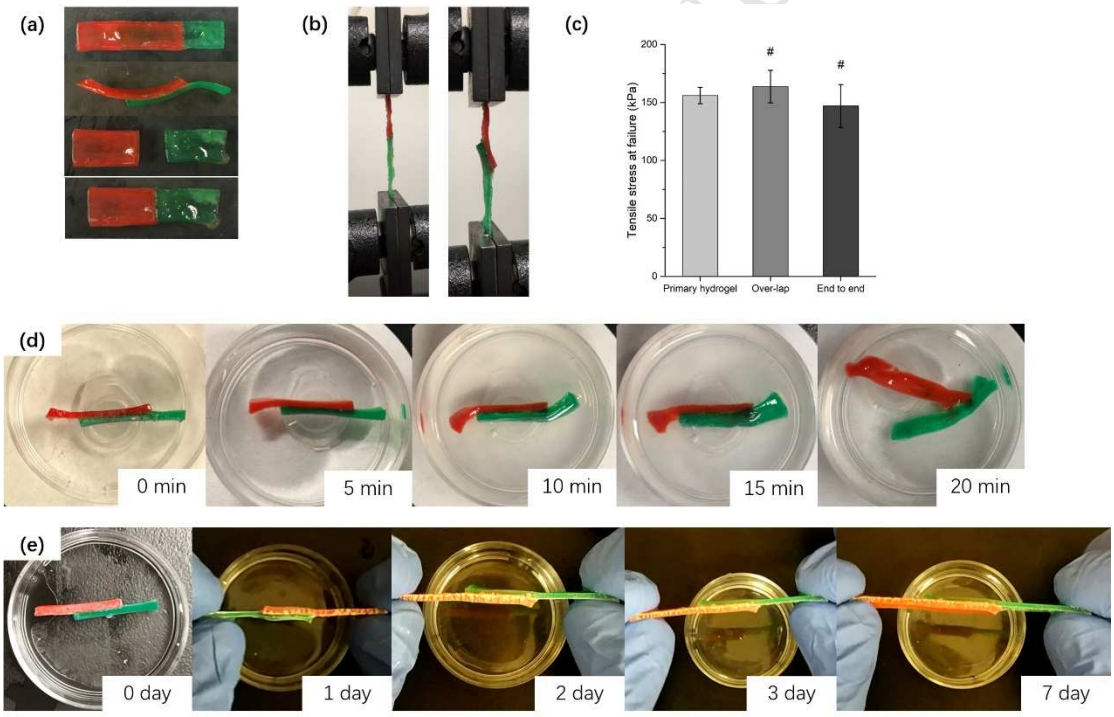

Fig. 5 (a) Self-healing models were demonstrated in two patterns: over-lap, and end to end. Tensile-adhesion measurements of healed hydrogels, the setup illustrations (b), and the tensile stress at failure (c) (# indicates no significant differences compared with primary GelMA hydrogel, $p > 0.05$, n=3). (d) Urea-mediated separation of the self-healed hydrogel, photographs were taken at the same intervals (5 min) until complete separation. (e) Self-healed GelMA-TA hydrogel immersed in PBS for seven days to demonstrate the water-resistant adhesion. Photographs were taken at day 0, 1, 2, 3 and 7 to

confirm the connections.

2.6 Cytocompatibility tests

We examined the cytocompatibility of GelMA-TA. Dermal fibroblast cells were cultured in a flat 96-well plate with or without the presence of GelMA-TA. Live/dead staining was performed to cells on day 1, 3, and 7 after seeding (Fig. 6a-f). Green fluorescence indicated living cells were found in all observations. Subsequently, we used cck8 quantitative detection of cell viability (Fig. 6g). Although the UV absorbance increases along with culture time from day 1 to 3 and 7 due to the proliferation of cells, there was no statistical difference in cell viability between two groups at the same time. These results suggested the hydrogel is applicable for *in vivo* use.

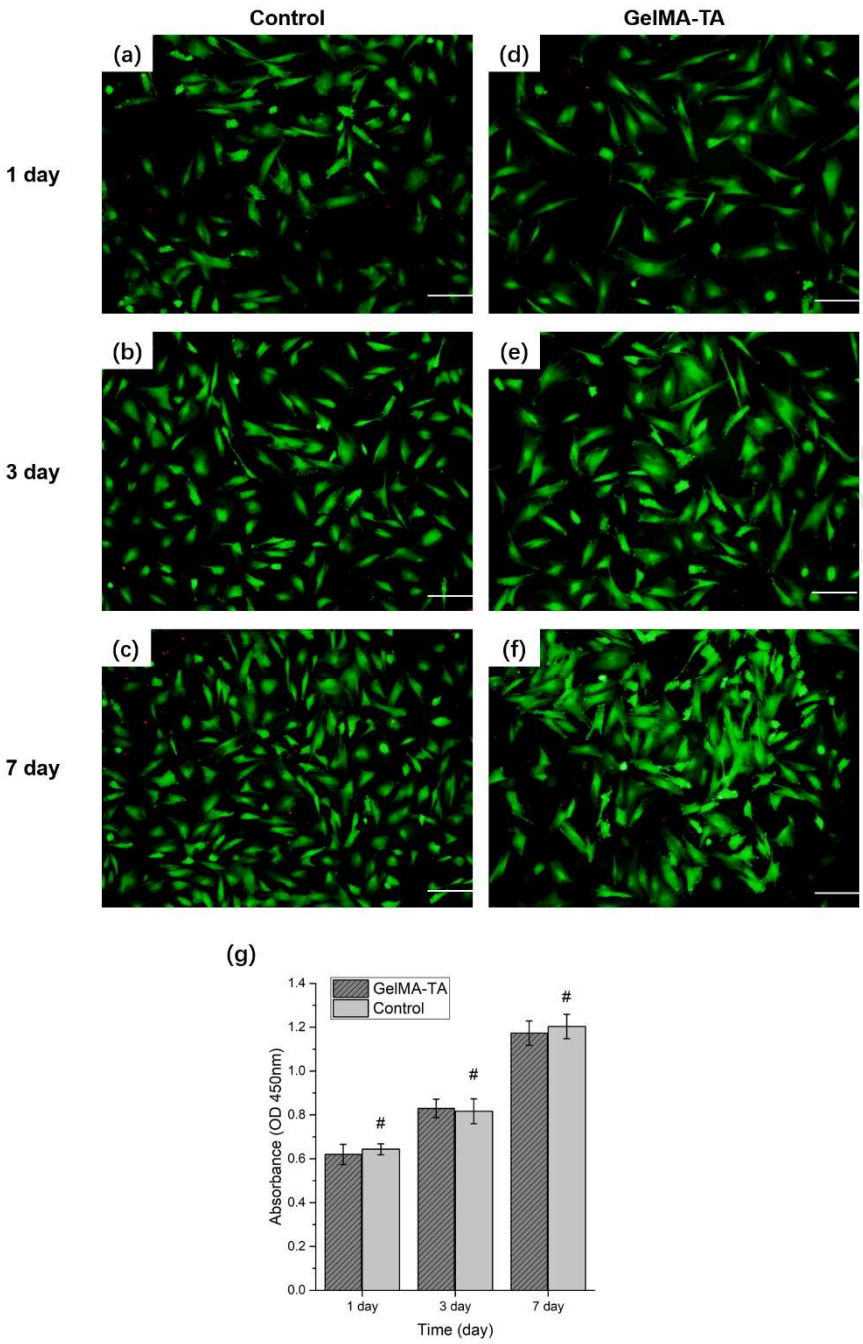

Fig. 6 Live/dead staining of dermal fibroblast cell cultured with or without (control) the GelMA-TA hydrogels. Fluorescent micrographs of the control group (a–c) and GelMA-TA group (d-f) on day 1, day 3 and day 7. Scale bars: 100 μm. (g) The proliferation of cells measured by CCK8 assays on days 1, 3 and 7. (# indicates no significant differences compared with the control, $p > 0.05$, n=3).

2.7 *in vivo* wound closure

As a wound dressing, dealing wounds with tension or in the moist environment are two common contexts.[64, 65] For these reasons, the olivary skin incision model in nude mice (Fig. 7a) and the gastric incision model in C57 mice (Fig. 8a) were designed. The curative effects were measured by a comprehensive comparison between three different treatments (no-operation, suture and hydrogel bonding) (Fig. 7a-c, 8a-c). Compared with surgical suture, one of the significant improvements of using adhesive hydrogels including the shortened and simplified operation procedure. Specifically, The adhesive hydrogels were placed over the incision where bilateral tissue aligned uniformly (Fig. 7c, 8c). After applying a gentle pressure for 1 min, the hydrogel offered adequate adhesion strength to address healing (Movie S4, Supporting Information).

Postoperative observations were described separately. Typical skin photos of three groups at seven days after surgery were taken. Among them, the worst healing effect was found in mice without any treatment (Fig. 7d). Due to the existence of tension, the repair of defect skin only depends on the migration of cells from the surrounding tissue. As a classic method, the wound in suture group closed completely. However, the secondary damage caused by surgical sutures were reflected in scar formation (Fig. 7e). In contrary to suture, GelMA-TA not only successfully closed the wound but also rendered a skin scar nearly invisible (Fig. 7f). The histological evaluations at 7th-day post operations were shown in Fig. 7g-i. Significant differences in the structure of healed skins can be seen between three groups. In general, normal skin comprising appendages can be divided into three layers including epidermis, dermis, and hypodermis (Fig. 7j). From this point of view, the wounds in the hydrogel treated group had the most complete and aligned structure retaining, whereas structural disorders of wound sites were evident in the other two groups. These results suggested that the tissue reconstruction was facilitated by GelMA-TA, which provided a noninvasive supporting for skin binding and repair.

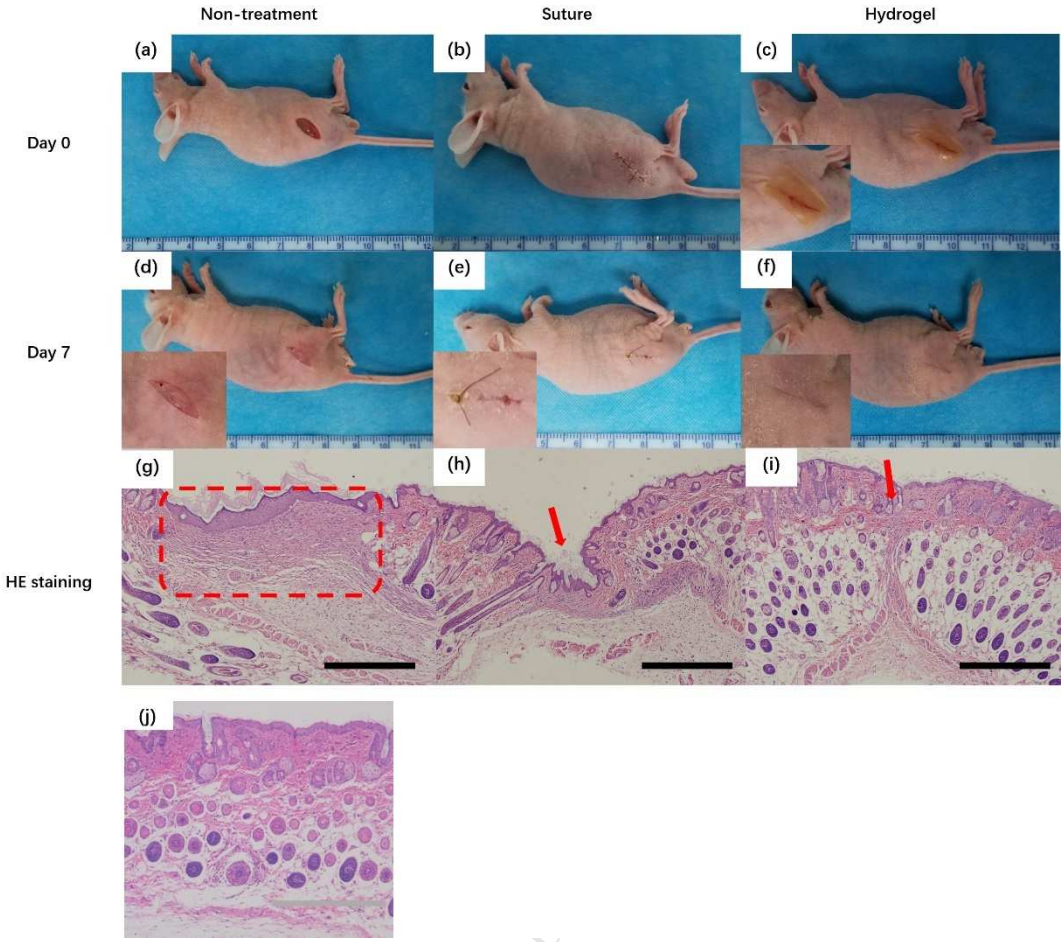

Fig.7 The healing of skin wound with tensile strength by using hydrogel adhesive and other two control methods. The labels of row and column are listed on the left and top, respectively. (a-c) Photographs of wound treatments. (d-f) Photographs of wounds 7 days postoperation. (g-i) Hematoxylin-eosin (HE) staining of healed skins. (j) Hematoxylin-eosin (HE) staining of non-wounded skin. Red dotted line and Red arrow indicate the wound. Scale bar = 500 μm

Each row or column of photos

Gastric models pose a greater challenge to the performances of adhesive hydrogel since its intraperitoneal working environment.[66, 67] The high mortality was found in the untreated group, four of six mice died within one week after surgery intervention, whereas the survival rate in other two groups was 100%. The general shape of stomachs after seven days was shown in Fig. 8d-f. In addition to the hydrogel-treated group, severe tissue adhesions were observed in other therapeutic groups, particularly in the no-sutured group where the leakage of gastric fluid caused inflammatory response not only resulted in the deformity and contracture of the stomach but also the extensive adhesion with surrounding tissue (Movie S5, Supporting Information). Histological observation revealed significant differences between the three groups in healing outcomes. In non-operation group (Fig. 8g), the typical

three-layer structure of gastric wall around the incision was disappeared, especially the large destruction of the mucosal layer. Mucosal ectropion alongside fistula formation suggesting that the tissue could not heal completely due to the prolonged inflammation phase. In the suture group (Fig. 8h), a classic fibroblast-mediated wound repair enabled to restore the tissue integrity. However, the structures of recovered stomach wall were disordered and replaced by distinct scar formation and intimal hyperplasia. Besides, excessive scars on the outmost surface of the stomach suggesting that their formation was related to tissue adhesion. In hydrogel group (Fig. 8i), the incision was entirely healed with precise edge opposition. Although the boundary between the serosal and muscular layers was blurred, this operation brought about the most uniform thickness of healing outcome. Also, we found immobilized fibroblast cells on both sides of the hydrogel, which is a standard interactive pattern when cells encounter with biocompatible materials. However, the presence of blank area in the middle of hydrogel clearly shown the autonomous status of two parts. Consequently, with the protection of GelMA-TA hydrogels, wound repairing took place independently to avoid annoying tissue adhesion.

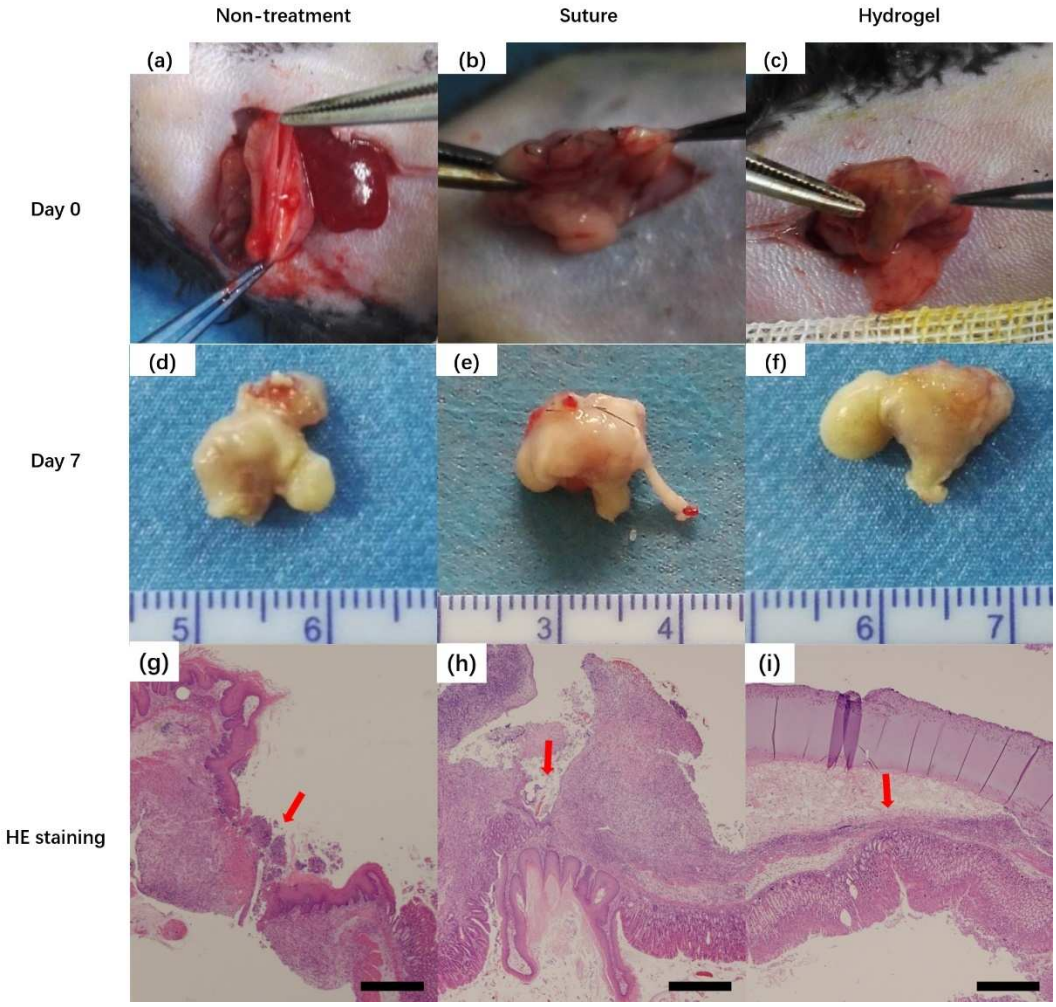

Fig.8 Gastric incision closure with the suture-free operation, and other two control groups. The labels of row and column are list on the left and top, respectively. (a-c) Intraoperative photographs. (d-f) Photographs of stomach specimens obtained one week after surgery. (g-i) Hematoxylin-eosin (HE) staining of the samples. Red arrows indicate the wounds. Scale bar = 500 μm

2.7. Applications as motion-sensor

As our hydrogel exhibiting sufficient mechanical strength, flexibility, and adhesiveness. We proposed a proof of concept study to explore GelMA-TA hydrogel as fundamental material of strain-sensor. Carbon Nanotubes (CNT) was selected as the conductive component since numerous CNT-based materials exhibit high electrical sensitivity and practicality.[68-71] As shown in Fig. S3a, by applying cyclic compression on the cylindrical gel, the luminance intensity of LED was synchronized responding to the dynamic pressure-driven resistance change (Movie S6, Supporting Information). We then employed thin cuboid hydrogels to capture the motions of the index finger. These strain-dependent behaviors were recorded in real-time by a multimeter (Fig. S3b, c). The normalized resistance ($R-R_0/R_0$, R_0: resting resistance and R: excitative resistance) curves waved stable along with the finger reciprocation in the same degree. Otherwise, shifts were distinct when bending angle altered. (Movie S7, Supporting Information). Notably, the broken hydrogel could spontaneously reconnect through the H-bond interaction (Fig. S4a), as well as the restoration of conductivity (Fig. S4b, c; Movie S8, Supporting Information).

3.Conclusion

We for the very first time incorporated TA into cross-linked GelMA to prepare structural reinforced hybrid hydrogels. All alluring features of the hydrogel are based on TA's ability to form intermolecular hydrogen bonding, which is simple but strong. GelMA-TA hydrogel with varied polymer contents can achieve superior mechanical properties in ultimate stress, compressive modulus, compressive strain and elongation to those of pristine GelMA. The highest deformability occurred with low concentrations of GelMA, and the high relative concentrations of TA to GelMA enhanced not only the structural stiffness of hydrogel but also the adhesion properties. Besides, this hydrogel exhibits excellent biocompatibility, which is a meaningful feature for wound dressing. In vivo experiments, these adhesive hydrogels achieved the best-recovered result in both skin and gastric wounds, exhibiting their clinical potentials under tension or wet conditions. Finally, we incorporated conductive CNTs into elastic GelMA-TA hydrogel, and the newly formed hydrogel was capable of sensing body motion. We believe this multifunctional hydrogel with physical properties that closely resemble nature tissue will expand our vision beyond

using protein-based hydrogels as cell incubators, but those innovative biomedical devices.

Materials and methods

Materials

Gelatin type A, tetramethylethylenediamine (TEMED), ammonium persulfate (APS), and methacrylic anhydride (MA) were purchased from Sigma. Tannic acid (TA) was obtained from Alfa Aesar. All chemicals were used without further purification.

Synthesis of Gelatin methacryloyl (GelMA).

We synthesized GelMA macromolecule with a methacryloyl graft by following the previous report.[43] Briefly, 10% (w/v) gelatin was completely dissolved in Dulbecco's phosphate-buffered saline (DPBS) at 50℃ with magnetic stirring. After that, MA (ratio: 0.8 ml MA/1 g gelatin) was added to the gelatin solution and stirred at 50℃ for 2 hours. The reaction was stopped by diluting the solution volume to 4-fold, and GelMA solution was dialyzed against deionized water with 12-14 cut-off at 50 ℃ for 1 week. Then the solution was lyophilized for 5 days, the product of white porous foam was stored at -20 ℃ until further use.

Fabrication of GelMA and GelMA-TA hydrogels

GelMA solutions were prepared by dissolving GelMA powder in deionized water with different concentrations (10%, 15%, 20% (w/v)) at 50 ℃ for 12 hours. TA storage solutions were prepared following the same procedure with the concentrations of 30%, 60%, 100% (w/v). The two-step method to synthesize the GelMA-TA hybrid hydrogels were briefed here. Firstly, GelMA hydrogel was formed by adding APS (5.7 mg ml^{-1}) and TEMED (2.9 mg ml^{-1}) into GelMA solution at 37 ℃ for a few minutes. After gelation, the hydrogels were immersed in TA solution for predetermined times, then the free TA was rinsed with deionized water. For compressive tests, cylindrical GelMA samples (7 mm height, 7 mm diameter) were produced. For tensile and self-healing tests, the block like GelMA samples (30 mm length, 10 mm width, and 2 mm thickness) were fabricated.

Rheology characterization.

All rheology experiments were implemented on a TA Discovery Hybrid Rheometer. The hydrogels (8mm in diameter and 1mm in thickness) were loaded on the parallel plate. During oscillation-frequency experiments, the samples were measured in the frequency ranging from 0.1 to 100 rad s^{-1} with a constant strain of 0.5% strain at room temperature.

FT-IR characterization

The intermolecular interaction between GelMA and TA were investigated by FTIR study. Lyophilized GelMA, TA, and GelMA-TA were respectively ground into powders and then mixed with KBr pellet to make specimens. The spectrums were obtained using an FTIR spectrometer (Nicolet Avtar 360, USA) at room temperature.

Mechanical tests

The mechanical properties of hydrogels were measured by an Instron 5965 mechanical analyzer. The compression tests were performed on cylindrical hydrogels at a speed of 10 mm/min to the maximum strain of 95%. The resilience tests were carried out five successive compression cycles up to 80% strain followed the same speed. For tensile tests, cuboid hydrogels were stretched at a speed of 20 mm/min to the breaking points. The compressive/tensile modulus was calculated as the slope in the linear region (0%-20%) from the stress-strain curves. All samples are coated with silicone oil to prevent moisture evaporation.

Volume changes

The relative volume (VC) of GelMA-TA hydrogels to the correspondingly pristine GelMA was calculated according to Equation: VC = V(GelMA-TA) / V(GelMA) × 100%, where the V(GelMA-TA) was obtained from different treatment conditions (30%, 60% and 100% w/v TA).

Swelling ratio

As-prepared GelMA or GelMA-TA hydrogels were incubated in PBS at 37 ^{o}C for 24h. Subsequently, the samples were taken out from solution and blotted with filter paper to remove free liquid and then recorded the weight as Ws. After lyophilization, the weight of hydrogels were recorded as Wd. The swelling ratio (SR) were calculated according to Equation: SR = Ws-Wd / Wd.

SEM characterization.

The lyophilized hydrogels were placed on a wafer for gold coating. The morphologies of samples were characterized by scanning electron microscope (JEOL-5900). The average pore size of hydrogels was analyzed by Image J software.

Adhesion tests

The experimental model to assess the shear adhesion strength on animal tissues was according to an established method,[72] by utilizing a universal testing machine (Instron 5965). Rectangular GelMA-TA or GelMA hydrogels (20 mm in length, 5 mm in width) were cut from bulk hydrogels and placed

uniformly between two porcine skin tissues (30 mm in length, 5 mm in width). TA solution was thinly applied on the porcine skin in same size as the control group. In the force-distance tests, GelMA-TA hydrogels with thicknesses (0.3 mm and 1 mm) were chosen. A 200 g external weight was applied to samples for 1 min to enhance the bonding. Afterward, tests were performed at a constant 10 mm/min speed of extension until the specimens were completely separated. Three samples of each group were tested, and the average strength was measured.

Self-healing model

To simulate the healing process for some *in vitro* measurements, hydrogels were stained with red and green pigments, respectively. The adhesion tests were performed in two configurations, overlap and end-to-end. Specifically, two hydrogels were joint by applying gentle pressure for 1 min. After then, we allowed hydrogel to undergo a further 6 h strengthening in the sealed petri dish. For the wet-resistant test, the whole healing process and observation period were carried out in PBS. Videos were taken on day 1, 2, 3, and 7, respectively. The PBS solution was changed daily.

In vitro cell viability study

Dermal-fibroblasts cells cultivation in 96-well plate with or without (control) the present of GelMA-TA hydrogels were used for cell viability studies. The relevant experiments were performed on days 1, 3, and 7, with the initial cells number 1×10^3 per well. The LIVE/DEAD kit (Invitrogen, USA) was used according to the instructions. After 15–20 min incubations at 37 ℃, the resultant images were obtained using a fluorescence microscope (IX71 FL, Olympus, Japan). For cell counting kit (CCK-8) test, 10 ml CCK-8 reagent was added to each well and cells were subsequently incubated at 37 ℃ for 1 h. The absorbance was measured at 450 nm using a multi-label counter (n = 3).

In vivo wound healing

Preparing for the in vivo applications, athymic mice and C57BL/6J mice (4–6 week-old) were purchased from the Experimental Animal Centre of Southern Medical University (Guangzhou, China). All animal experiments are subject to animal care institution and approved by the Ethics Committee.

For the experiment of athymic mice skin tension wound closure, eighteen mice were randomly divided into 3 groups and anesthetized with pentobarbital sodium (1.3 mg kg^{-1}). The tension incision model was made by removing a piece of olivary full-thickness skin around 1 cm in length. The GelMA-TA hydrogels (20 mm×15 mm×1 mm) was subsequently applied to cover the incision site with 1 min gently external pressure. Non-treatment group and

suture group (using a 4-0 PROLENE) were set as the control groups. One week after operations, the healing outcomes were first recorded by photos, after that the tissue specimens were fixed by 4% paraformaldehyde for further hematoxylin and eosin (HE) staining. The histological observation of incision sites was evaluated via a microscope (IX71 FL, Olympus, Japan).

For the experiment of sutureless gastric incision closure, most of the operations were same as above, with only several modifications. The C57BL/6J mice were fasted 24 hours before surgery, and the hair of mice was denuded in a range from chest to the lower abdomen after anesthetization. The length of each mouse's stomach incision was approximately 1 cm.

Strain-sensitive conductivity of GelMA-TA hydrogels

The same procedures and dimensions were followed to prepare conductive hydrogels except that CNTs (5mg/ml) was added to GelMA solution before gelation.

For pressure-sensitive test: The experimental setup included Instron 5965 mechanical analyzer to perform a cyclic compression test and light-emitting diode (LED) as an indicator. The entire hydrogel-LED circuit was insulated from the frame of the machine. Therefore, the resistance variations of hydrogel along with compressing reflected in LED's luminance intensity change. The compressive tests were carried out at a speed of 10 mm/min with the strain up to 80%.

For finger movement capture: The rectangular hydrogel was sealed between two PDMS films and was connected to conductive guide wire at both ends. The device was subsequently attached to the proximal interphalangeal (PIP) joint of index finger. These strain-dependent behaviors were recorded (resistance) in real-time by the two-probes digital multimeter.

To test whether the conductivity of hydrogel restored after self-healing, the initial volume (before the treatment of TA) of hydrogels was 7 mm in height and 20 mm in diameter. The conductivity of the reconnected hydrogel was first illustrated by the LED-based verification device, and then had a quantifiable conductive evaluation between pristine and recovered hydrogels. The conductivity (σ) was calculated from the equation $\sigma=1/\rho$, where the resistivity (ρ) were measured using a digital four-probe tester (ST-2258C Suzhou Jingge Electronic Co., Ltd.), with a linear probe head (2.0 mm).

Statistical analysis

One-way analysis of variance (ANOVA) with a 95% confidence interval was applied to evaluate the difference between two groups using SPSS18.0 software. All data derived from three independent experiments. When p-value less than 0.05, the difference was considered to be statistically significant. All graphs were plotted using OriginPro 2016 software (Northampton, MA).

[1] Annabi N, Tamayol A, Uquillas JA, Akbari M, Bertassoni LE, Cha C, et al. 25th anniversary article: rational design and applications of hydrogels in regenerative medicine. Advanced Materials. 2014;26:85-124.

[2] Kopeček J. Hydrogel biomaterials: a smart future? Biomaterials. 2007;28:5185-92.

[3] Zhang YS, Khademhosseini A. Advances in engineering hydrogels. Science. 2017;356.

[4] Caló E, Khutoryanskiy VV. Biomedical applications of hydrogels: A review of patents and commercial products. European Polymer Journal. 2015;65:252-67.

[5] Liu Y, Chan-Park MB. A biomimetic hydrogel based on methacrylated dextran-graft-lysine and gelatin for 3D smooth muscle cell culture. Biomaterials. 2010;31:1158-70.

[6] Ifkovits JL, Burdick JA. Review: photopolymerizable and degradable biomaterials for tissue engineering applications. Tissue engineering. 2007;13:2369-85.

[7] Lynn A, Yannas I, Bonfield W. Antigenicity and immunogenicity of collagen. Journal of Biomedical Materials Research Part B: Applied Biomaterials. 2004;71:343-54.

[8] Gorgieva S, Kokol V. Collagen-vs. gelatine-based biomaterials and their biocompatibility: review and perspectives: INTECH open access publisher Croatia; 2011.

[9] Reddy N, Reddy R, Jiang Q. Crosslinking biopolymers for biomedical applications. Trends in biotechnology. 2015;33:362-9.

[10] Mironi-Harpaz I, Wang DY, Venkatraman S, Seliktar D. Photopolymerization of cell-encapsulating hydrogels: crosslinking efficiency versus cytotoxicity. Acta biomaterialia. 2012;8:1838-48.

[11] Yue K, Trujillo-de Santiago G, Alvarez MM, Tamayol A, Annabi N, Khademhosseini A. Synthesis, properties, and biomedical applications of gelatin methacryloyl (GelMA) hydrogels. Biomaterials. 2015;73:254-71.

[12] Klotz BJ, Gawlitta D, Rosenberg AJ, Malda J, Melchels FP. Gelatin-Methacryloyl Hydrogels: Towards Biofabrication-Based Tissue Repair. Trends Biotechnol. 2016;34:394-407.

[13] Nichol JW, Koshy ST, Bae H, Hwang CM, Yamanlar S, Khademhosseini A. Cell-laden microengineered gelatin methacrylate hydrogels. Biomaterials. 2010;31:5536-44.

[14] Van Den Bulcke AI, Bogdanov B, De Rooze N, Schacht EH, Cornelissen M, Berghmans H. Structural and rheological properties of methacrylamide modified gelatin hydrogels. Biomacromolecules. 2000;1:31-8.

[15] Koshy ST, Ferrante TC, Lewin SA, Mooney DJ. Injectable, porous, and cell-responsive gelatin cryogels. Biomaterials. 2014;35:2477-87.

[16] Cha C, Shin SR, Gao X, Annabi N, Dokmeci MR, Tang XS, et al. Controlling mechanical properties of cell-laden hydrogels by covalent incorporation of graphene oxide. Small. 2014;10:514-23.

[17] Shin SR, Zihlmann C, Akbari M, Assawes P, Cheung L, Zhang K, et al. Reduced Graphene Oxide-GelMA Hybrid Hydrogels as Scaffolds for Cardiac Tissue Engineering. Small. 2016;12:3677-89.

[18] Hassanzadeh P, Kazemzadeh-Narbat M, Rosenzweig R, Zhang X, Khademhosseini A, Annabi N, et al. Ultrastrong and flexible hybrid hydrogels based on solution self-assembly of chitin nanofibers in gelatin methacryloyl (GelMA). J Mater Chem B. 2016;4:2539-43.

[19] Xiao W, He J, Nichol JW, Wang L, Hutson CB, Wang B, et al. Synthesis and characterization of photocrosslinkable gelatin and silk fibroin interpenetrating polymer network hydrogels. Acta Biomater. 2011;7:2384-93.

[20] Levett PA, Melchels FP, Schrobback K, Hutmacher DW, Malda J, Klein TJ. A biomimetic extracellular matrix for cartilage tissue engineering centered on photocurable gelatin, hyaluronic acid and chondroitin sulfate. Acta biomaterialia. 2014;10:214-23.

[21] Qi H, Du Y, Wang L, Kaji H, Bae H, Khademhosseini A. Patterned differentiation of individual embryoid bodies in spatially organized 3D hybrid microgels. Advanced materials. 2010;22:5276-81.

[22] Kolesky DB, Truby RL, Gladman A, Busbee TA, Homan KA, Lewis JA. 3D bioprinting of vascularized, heterogeneous cell‐laden tissue constructs. Advanced materials. 2014;26:3124-30.

[23] Zuo Y, Liu X, Wei D, Sun J, Xiao W, Zhao H, et al. Photo-cross-linkable methacrylated gelatin and hydroxyapatite hybrid hydrogel for modularly engineering biomimetic osteon. ACS applied materials & interfaces. 2015;7:10386-94.

[24] Taylor DL, In Het Panhuis M. Self-Healing Hydrogels. Adv Mater. 2016;28:9060-93.

[25] Waite JH, Tanzer ML. Polyphenolic substance of Mytilus edulis: novel adhesive containing L-dopa and hydroxyproline. Science. 1981;212:1038-40.

[26] Lee H, Dellatore SM, Miller WM, Messersmith PB. Mussel-inspired surface chemistry for multifunctional coatings. science. 2007;318:426-30.

[27] Ud‐Din S, Volk SW, Bayat A. Regenerative healing, scar‐free healing and scar formation across the species: current concepts and future perspectives. Experimental dermatology. 2014;23:615-9.

[28] Sahiner N, Sagbas S, Sahiner M, Silan C, Aktas N, Turk M. Biocompatible and biodegradable poly(Tannic Acid) hydrogel with antimicrobial and antioxidant properties. Int J Biol Macromol.

2016;82:150-9.

[29] Kozlovskaya V, Xue B, Lei W, Padgett LE, Tse HM, Kharlampieva E. Hydrogen‐Bonded Multilayers of Tannic Acid as Mediators of T‐Cell Immunity. Advanced healthcare materials. 2015;4:686-94.

[30] Dierendonck M, Fierens K, De Rycke R, Lybaert L, Maji S, Zhang Z, et al. Nanoporous Hydrogen Bonded Polymeric Microparticles: Facile and Economic Production of Cross Presentation Promoting Vaccine Carriers. Advanced Functional Materials. 2014;24:4634-44.

[31] Erel-Unal I, Sukhishvili SA. Hydrogen-bonded multilayers of a neutral polymer and a polyphenol. Macromolecules. 2008;41:3962-70.

[32] Le Bourvellec C, Renard CM. Interactions between polyphenols and macromolecules: quantification methods and mechanisms. Crit Rev Food Sci Nutr. 2012;52:213-48.

[33] Chen YN, Peng L, Liu T, Wang Y, Shi S, Wang H. Poly(vinyl alcohol)-Tannic Acid Hydrogels with Excellent Mechanical Properties and Shape Memory Behaviors. ACS Appl Mater Interfaces. 2016;8:27199-206.

[34] Shin M, Kim K, Shim W, Yang JW, Lee H. Tannic Acid as a Degradable Mucoadhesive Compound. ACS Biomaterials Science & Engineering. 2016;2:687-96.

[35] Kim K, Shin M, Koh MY, Ryu JH, Lee MS, Hong S, et al. TAPE: A medical adhesive inspired by a ubiquitous compound in plants. Advanced Functional Materials. 2015;25:2402-10.

[36] Shin M, Ryu JH, Park JP, Kim K, Yang JW, Lee H. DNA/Tannic Acid Hybrid Gel Exhibiting Biodegradability, Extensibility, Tissue Adhesiveness, and Hemostatic Ability. Advanced Functional Materials. 2015;25:1270-8.

[37] Fan H, Wang L, Feng X, Bu Y, Wu D, Jin Z. Supramolecular Hydrogel Formation Based on Tannic Acid. Macromolecules. 2017;50:666-76.

[38] Ahn BK, Lee DW, Israelachvili JN, Waite JH. Surface-initiated self-healing of polymers in aqueous media. Nat Mater. 2014;13:867-72.

[39] Li L, Yan B, Yang J, Chen L, Zeng H. Novel mussel-inspired injectable self-healing hydrogel with anti-biofouling property. Adv Mater. 2015;27:1294-9.

[40] Han L, Lu X, Wang M, Gan D, Deng W, Wang K, et al. A Mussel‐Inspired Conductive, Self‐Adhesive, and Self‐Healable Tough Hydrogel as Cell Stimulators and Implantable Bioelectronics. Small. 2017;13.

[41] Liu Y, Xu K, Chang Q, Darabi MA, Lin B, Zhong W, et al. Highly Flexible and Resilient Elastin Hybrid Cryogels with Shape Memory, Injectability, Conductivity, and Magnetic Responsive Properties. Advanced Materials. 2016;28:7758-67.

[42] Shin SR, Jung SM, Zalabany M, Kim K, Zorlutuna P, Kim SB, et al. Carbon-nanotube-embedded hydrogel sheets for engineering cardiac constructs and bioactuators. ACS nano. 2013;7:2369-80.

[43] Zhao X, Lang Q, Yildirimer L, Lin ZY, Cui W, Annabi N, et al.

Photocrosslinkable Gelatin Hydrogel for Epidermal Tissue Engineering. Adv Healthc Mater. 2016;5:108-18.

[44] Kozlovskaya V, Kharlampieva E, Drachuk I, Cheng D, Tsukruk VV. Responsive microcapsule reactors based on hydrogen-bonded tannic acid layer-by-layer assemblies. Soft Matter. 2010;6:3596-608.

[45] Coleman MM, Lee KH, Skrovanek DJ, Painter PC. Hydrogen bonding in polymers. 4. Infrared temperature studies of a simple polyurethane. Macromolecules. 1986;19:2149-57.

[46] Jastrzebska M, Zalewska-Rejdak J, Wrzalik R, Kocot A, Mroz I, Barwinski B, et al. Tannic acid-stabilized pericardium tissue: IR spectroscopy, atomic force microscopy, and dielectric spectroscopy investigations. J Biomed Mater Res A. 2006;78:148-56.

[47] Topkaya SN. Gelatin methacrylate (GelMA) mediated electrochemical DNA biosensor for DNA hybridization. Biosensors and Bioelectronics. 2015;64:456-61.

[48] Barrett DG, Fullenkamp DE, He L, Holten‐Andersen N, Lee KYC, Messersmith PB. pH‐Based Regulation of Hydrogel Mechanical Properties Through Mussel‐Inspired Chemistry and Processing. Advanced functional materials. 2013;23:1111-9.

[49] Shin H, Olsen BD, Khademhosseini A. The mechanical properties and cytotoxicity of cell-laden double-network hydrogels based on photocrosslinkable gelatin and gellan gum biomacromolecules. Biomaterials. 2012;33:3143-52.

[50] Chen YC, Lin RZ, Qi H, Yang Y, Bae H, Melero-Martin JM, et al. Functional Human Vascular Network Generated in Photocrosslinkable Gelatin Methacrylate Hydrogels. Adv Funct Mater. 2012;22:2027-39.

[51] Kong HJ, Wong E, Mooney DJ. Independent control of rigidity and toughness of polymeric hydrogels. Macromolecules. 2003;36:4582-8.

[52] Silver FH, Freeman JW, DeVore D. Viscoelastic properties of human skin and processed dermis. Skin research and technology. 2001;7:18-23.

[53] Han L, Lu X, Liu K, Wang K, Fang L, Weng L-T, et al. Mussel-Inspired Adhesive and Tough Hydrogel Based on Nanoclay Confined Dopamine Polymerization. ACS nano. 2017;11:2561-74.

[54] Zhang X, Do MD, Casey P, Sulistio A, Qiao GG, Lundin L, et al. Chemical modification of gelatin by a natural phenolic cross-linker, tannic acid. J Agric Food Chem. 2010;58:6809-15.

[55] Zhang X, Do MD. Plasticization and crosslinking effects of acetone-formaldehyde and tannin resins on wheat protein-based natural polymers. Carbohydr Res. 2009;344:1180-9.

[56] Jing X, Mi H-Y, Napiwocki BN, Peng X-F, Turng L-S. Mussel-inspired electroactive chitosan/graphene oxide composite hydrogel with rapid self-healing and recovery behavior for tissue engineering. Carbon. 2017;125:557-70.

[57] Benton JA, DeForest CA, Vivekanandan V, Anseth KS.

Photocrosslinking of gelatin macromers to synthesize porous hydrogels that promote valvular interstitial cell function. Tissue Engineering Part A. 2009;15:3221-30.

[58] Chen YC, Lin RZ, Qi H, Yang Y, Bae H, Melero‐Martin JM, et al. Functional human vascular network generated in photocrosslinkable gelatin methacrylate hydrogels. Advanced functional materials. 2012;22:2027-39.

[59] Xu K, Liu Y, Bu S, Wu T, Chang Q, Singh G, et al. Egg Albumen as a Fast and Strong Medical Adhesive Glue. Adv Healthc Mater. 2017;6.

[60] Ghobril C, Grinstaff M. The chemistry and engineering of polymeric hydrogel adhesives for wound closure: a tutorial. Chemical Society Reviews. 2015;44:1820-35.

[61] Phadke A, Zhang C, Arman B, Hsu C-C, Mashelkar RA, Lele AK, et al. Rapid self-healing hydrogels. Proceedings of the National Academy of Sciences. 2012;109:4383-8.

[62] Ryu JH, Lee Y, Kong WH, Kim TG, Park TG, Lee H. Catechol-functionalized chitosan/pluronic hydrogels for tissue adhesives and hemostatic materials. Biomacromolecules. 2011;12:2653-9.

[63] Wang R, Li J, Chen W, Xu T, Yun S, Xu Z, et al. A Biomimetic Mussel‐Inspired ε‐Poly‐l‐lysine Hydrogel with Robust Tissue‐Anchor and Anti‐Infection Capacity. Advanced Functional Materials. 2017;27.

[64] Boateng JS, Matthews KH, Stevens HN, Eccleston GM. Wound healing dressings and drug delivery systems: a review. Journal of pharmaceutical sciences. 2008;97:2892-923.

[65] Annabi N, Tamayol A, Shin SR, Ghaemmaghami AM, Peppas NA, Khademhosseini A. Surgical materials: current challenges and nano-enabled solutions. Nano today. 2014;9:574-89.

[66] Jiang J, Wan W, Ge L, Bu S, Zhong W, Xing M. Mussel-inspired nanofibrous sheet for suture-less stomach incision surgery. Chemical Communications. 2015;51:8695-8.

[67] Okamura Y, Kabata K, Kinoshita M, Saitoh D, Takeoka S. Free-Standing Biodegradable Poly(lactic acid) Nanosheet for Sealing Operations in Surgery. Adv Mater. 2009;21:4388-92.

[68] Shin MK, Oh J, Lima M, Kozlov ME, Kim SJ, Baughman RH. Elastomeric conductive composites based on carbon nanotube forests. Advanced Materials. 2010;22:2663-7.

[69] Lipomi DJ, Vosgueritchian M, Tee BC, Hellstrom SL, Lee JA, Fox CH, et al. Skin-like pressure and strain sensors based on transparent elastic films of carbon nanotubes. Nature nanotechnology. 2011;6:788-92.

[70] Darabi MA, Khosrozadeh A, Wang Q, Xing M. Gum sensor: a stretchable, wearable, and foldable sensor based on carbon nanotube/chewing gum membrane. ACS applied materials & interfaces. 2015;7:26195-205.

[71] Xu J, Wang S, Wang G-JN, Zhu C, Luo S, Jin L, et al. Highly stretchable polymer semiconductor films through the nanoconfinement

effect. Science. 2017;355:59-64.

[72] Kull S, Martinelli I, Briganti E, Losi P, Spiller D, Tonlorenzi S, et al. Glubran2 surgical glue: in vitro evaluation of adhesive and mechanical properties. Journal of Surgical Research. 2009;157:e15-e21.